UNIVERSITY OF LA LAGUNA

MASTER's Degree in ASTROPHYSICS

MASTER's Degree Thesis

THE STAR FORMATION HISTORY IN CONSTRAINED LOCAL GROUP SIMULATIONS

Supervisors

Dr. ARIANNA DI CINTIO

Prof. CHRISTOFER BROOK

Candidate

RUBEN BELMEZ ORELLANA

JULY 2020

Abstract

Debido a que las galaxias consideradas "enanas" son las más abundantes en el universo, resulta muy revelador conocer la física detrás de ellas ya que los procesos que experimentan son los más abundantes y fácilmente detectables. Respecto al Grupo Local, hay una característica de las mencionadas galaxias, conocida gracias a las observaciones, que no es correctamente explicada por los modelos teóricos y esta es la formación estelar que ha experimentado la galaxia en su historia (siendo el caso de ser muy rápida y corta para algunas galaxias y lenta y más prolongada en el tiempo para otras), cuyas observaciones indican que no todas las galaxias consideradas enanas han tenido la misma formación estelar. En este punto es importante indicar que el mencionado objetivo de estudio de dichas galaxias parte de los progresos realizados por investigaciones anteriores, Gallart et al. 2015 y Bermejo-Climent et al. 2018, cuyos avances sirven como punto de partida para este trabajo. Estos trabajos previos concluyeron que las causas de las discrepancias de la teoría con las observaciones podrían tener su origen en la época en la cual cada una de las galaxias fue formada, creando a su vez unas etiquetas ("lentas" y "rápidas") con las que poder seleccionar las galaxias según su formación estelar particular, esta clasificación se basa simplemente en considerar que una galaxia se consideraría "rápida" de haber formado una cantidad significativa de sus estrellas no más tarde de $z = 2$, concluyéndose para el término "lenta" aquella que formó la mayor parte de sus estrellas después de $z = 2$, en este trabajo tomamos como "cantidad significativa" el valor del 50%. El objetivo de este trabajo es verificar las hipótesis realizadas por trabajos previos en base a sus descubrimientos, comprobando si se puede establecer que el entorno de las galaxias en la época de su formación tuvo un impacto real en la formación estelar final de la galaxia.

Debido a que este trabajo tiene un punto de vista teórico, la fuente principal de información que se va a emplear en una serie de simulaciones cosmológicas hidrodinámicas denominada CLUES, construidas bajo el modelo cosmológico concordante ΛCDM. Este grupo de simulaciones tiene varias características siendo probablemente la más importante que son simulaciones donde las observaciones se han incluido como parámetros en las condiciones iniciales con el fin de ser capaz de reproducir el Grupo Local observado, la forma en la que las mencionadas observaciones son añadidas se puede resumir en forzando las escalas del universo conocidas a tener los valores que garanticen dichas observaciones (escalas por debajo de $2h^{-1}$ Mpc). Además, estas simulaciones están divididas en dos "grupos", el primero, encargado de reproducir el denominado Universo Local (que se puede resumir como nuestro vecindario en términos de cúmulos de galaxias), simulación puramente

gravitatoria donde se han incluido únicamente particulas de materia oscura, en un volumen de lado $160h^{-1}$ Mpc. En el segundo grupo de simulaciones, donde se han incluido partículas bariónicas (además de su física asociada), es una ampliación en detalle (en un volumen más pequeño de lado $64h^{-1}$ Mpc) de los candidatos prometedores a Grupo Local. Estos "candidatos prometedores" vienen de las particularidades de las condiciones iniciales ya que, por un lado, estas se establecen mediante realizaciones de campos gaussianos aleatorios (los cuales se han dejado evolucionar de $z = 50$ hasta el presente $z = 0$) y, por otro lado, se buscan en dichas realizaciones los cúmulos que guarden mayores similitudes con el Grupo Local real, siendo el más parecido de entre ellos el elegido para las condiciones iniciales definitivas. Una vez que se han encontrado las condiciones iniciales adecuadas para reproducir las observaciones, se pone en marcha la simulación completa, partiendo del tiempo correspondiente a $z = 6$ hasta el presente $z = 0$, configurada bajo los conjuntos de parámetros cosmológicos WMAP3 y WMAP5, aunque en este trabajo se usará el primer grupo cuyos parámetros son: $\Omega_m = 0.24$, $\Omega_b = 0.042$, $\Omega_\Lambda = 0.76$, un valor de normalización de $\sigma_8 = 0.73$ y una pendiente para el espectro de potencias $n = 0.95$.

El grupo de galaxias elegidas para el estudio son aquellas que en el tiempo presente cumplen que, por un lado, no son ninguna de las galaxias más masivas del Grupo Local (Andrómeda o la Vía Láctea) y, por otro lado, están fuera del radio virial de estas dos, es decir, no han sido absorbidas por ninguna de estas, de esta manera puede asegurarse más fácilmente que los cambios que las galaxias hayan sufrido no están causados por haber caído en la influencia gravitatoria de galaxias más masivas. Se ha rastreado cada una de las 42 galaxias seleccionadas a lo largo de una media de 13 pasos temporales de la simulación, las principales magnitudes y características que se han intentado estudiado en cada uno de esos pasos temporales han sido la masa total de la galaxia, la densidad de masa (incluyendo todos los tipos de partículas) entre 1 y 5 veces el radio virial de dicha galaxia y la misma densidad pero en una esfera de 1 Mpc de radio. Una vez obtenidas todas las mencionadas magnitudes de cada galaxia en cierto número de pasos temporales se ha analizando dicha información centrándose en las siguientes propiedades: primero, estudiar el ritmo de acreción de masa de las galaxias, es decir, como ha aumentado su masa total con el tiempo para identificar qué periodo fue el más relevante en términos de formación estelar. Segundo, intentar clasificar las galaxias según la densidad entre 1 y 5 radios viriales, además de por intervalos de masa total 10^{6-7} $M_\odot$, 10^{7-8} $M_\odot$ y 10^{8-9} $M_\odot$, para intentar correlar épocas de formación estelar con periodos de sobredensidad en varios tiempos de la simulación.

Los resultados apuntan a que la sobredensidad de cada galaxia sí que tuvo su influencia con épocas importantes de formación estelar, ya que se observa ritmos de

acreción de masa mayores para las denominadas galaxias "rápidas", las cuales tienen en general sobredensidades más altas en comparación con las galaxias "lentas". Estas conclusiones se cumplen especialmente en tiempos más lejanos donde se podría presuponer que las galaxias no han tenido demasiado tiempo de interactuar con el entorno o con otras galaxias, para tiempos más presentes es más complicado observar las implicaciones exclusivas de una posible sobredensidad ya que las galaxias han empezado a sufrir interacciones, cuyas implicaciones se mezclan su propia evolución.

Table of Contents

List of Tables

List of Figures

Chapter 1

Introduction

Dwarf galaxies are the most abundant galaxies in the universe, so understanding the physics behind them, their properties and the evolution of them, is mandatory in order to better understand and model the galactic and extra galactic astrophysics. In terms of classification, previous research works based on observational properties (i.e. the stellar population and the gas content), established that dwarf galaxies could be separated roughly in three groups: dwarf spheroidal (*dSph*), which have little or no gas at all and are not forming stars any more (they are quenched), dwarf irregulars (*dIrr*) as the opposite case to the spheroidal ones, they are rich in gas and keep forming stars for a longer period of time and finally the transition type (*dT*), whose properties settle in the middle of both of the previous types, as the name itself suggests.

As mentioned, the previous classification is derived from the observational study of the properties of the galaxies (such as the location, the gas content, the star formation history, etc.) and, although there are plenty of hypothesis, the origin of these differences is not yet well explained. A particular theoretical approach for solving the mystery, by *Gallart et al. 2015*, tried to explain these differences focusing on the separate evolutionary paths that each galaxy (or better said, each group of galaxies in terms of classification) took and what could led to explain the origin of the different gas content between galaxies in the present, considering ram-pressure, tidal stripping and other interactions galaxy-galaxy or galaxy-cluster as the main actors in explaining the mentioned gas content difference. Although it seems reasonable to assume that the evolution that each galaxy had made its impact on the present properties, it seems that it is not enough to give a solid answer to this problem, especially because this argument requires the assumption that the end of the star forming periods were mainly caused by the loss of gas of the galaxy at some moment of their evolution, which almost neglects the consideration that the surroundings of the galaxy in its earlier stages had any key role.

The previous projects strongly hint to the fact, as suggested in *Gallart et al. 2015*, that the environment of the galaxy in the early stages of its history had a relevant impact on the evolutionary path it would eventually follow and, consequently, the current properties that the galaxies have. Here lies the purpose of this work, shedding light on that hint and check more deeply if there really is a correlation between the environment in which the dwarf galaxies were assembled and their final classification, roughly. The discrimination method we have used to label the galaxies is not the previously introduced (based on observational properties) but one joining the work made by *Gallart et al. 2015* with *Bermejo-Climent et al. 2018*, this difference is established basically in checking if galaxies have formed a significant fraction of their total amount of stars (we use the limit of 50%) by $z = 2$. If a galaxy has formed the vast majority of the stars before $z = 2$ is considered a *fast* dwarf and, however, if most stars were form after $z = 2$ it will be considered a *slow* dwarfs.

The data source for this work is the CLUES simulation (*Gottloeber et al. 2010*), which will be introduced more deeply in the following section. One of the most important tools to make the discrimination for the selected target galaxies is their star formation history (SFH henceforth), through it is possible to check quantitatively how were the star formation rates of galaxies throughout their lifetime and makes easier to label them as *fast* dwarfs or *slow* dwarfs. Qualitatively, using the available information about the properties of the stellar population helps the labelling of the galaxies be more precise. Adding the information coming from the SFH with making several images of all the matter content distribution for each target galaxy can provide a considerable preliminary hint of the main responsible of the fate of the galaxies even before making a proper analysis.

Once the classification is adequately settled and the present day properties of every target galaxy are known, each galaxy can be traced back in time until a relevant early stage of its life. For our work, that relevant early time is the specific time (or the closest time available) when each galaxy form the 50% of their stars, in the end the time that decides whether the selected galaxy is a *fast* dwarf or a *slow* dwarf. By doing so we can check, for several redshifts between $z = 0$ and the 50% star formation redshift of each galaxy, the evolution of the environment in density considering all types of matter particles present in the simulation: dark matter, gas and stars. This procedure allows the possibility to correlate the evolutionary paths of the dwarfs and the current properties with an early stage environmental characteristics and the evolution of it.

Chapter 2

CLUES Simulation

The Local Group, our galactic neighbourhood, is the most studied and best understood region of the universe, for obvious reasons, and so it can be considered some sort of "cosmic laboratory" where the existing cosmological models and the new hypothesis can "moderately easy" be tested, this is what is called the *near field cosmology*.

The Local Group has been the training ground of most theories in astrophysics and cosmology (among other areas), such as the galaxy formation recipes (just to mention one), built under the current concordant cosmological model, the so called ΛCDM model (*Peebles 1998*). This model is based on a matter-energy content of baryons and Cold Dark Matter dominated by a cosmological constant (the Λ term), the model also tells about the expansion history, the initial conditions and the mentioned material content. The predictive power of the theory shows up alongside the framework composed by its own content added to the physical laws that rule the dark matter, baryons and radiation.

Numerical simulations allow the study of the universe in diverse scales, both for distances and masses, which can provide with a detailed understanding further than where observations can currently reach, naturally ensuring that the model represented is accurate enough. Following with aforementioned, if the potential of the numerical simulations can be added with the detailed understanding of the Local Group through the observations a useful and powerful tool can be obtained, as it has the power and predictive power of a simulation and the accuracy of the observations. This lead us to the group of simulations we use in this work, Constrained Local UniversE Simulations (CLUES) (*Gottloeber et al. 2010*), a series of constrained cosmological numerical hydrodynamical simulations which are designed to reproduce the observed large scale structure of the Local Group and its neighbourhood: the close clusters, the cosmic web, etc. (the so called Local

Universe).

2.1 Initial Conditions

As mentioned, observational data was incorporated to CLUES simulations as constrains which make available for the simulations to reproduce accurately the observed nearby universe on scales larger that $\approx 5h^{-1}$Mpc (*Klypin et al. 2003*), leaving the structure at smaller scales unaffected by the constrains, what make them random. The observational data comes from two different sources. The first one is a set of radial velocities of galaxies taken from Mark III Catalog of Galaxy Peculiar Velocities (*Willick et al. 1997*), surface brightness fluctuation (SBF) survey (*Tonry et al. 2001*) and the Karachentsev (*Karachentsev et al. 2004*) catalogs. Peculiar velocities of this source are less affected by the non-linear effects of the cosmological structure evolution and they are used as constrains as mere linear quantities. The second source of observations is the catalog of X-ray near clusters of galaxies (*Reiprich and Böhringer 2002*), obtaining the overdensity of a cluster knowing its virial parameters and assuming a top-hat model, the knowledge of this overdensity can be then imposed as a constrain of the mass scale of the cluster.

In order to incorporate that information into the initial conditions, the Hoffman-Ribak (*Hoffman and Ribak 1991*) algorithm is used to generate realizations of Gaussian random fields on a 256^3 particle uniform mesh, these realizations are used to constrain the observational data. A problem arises here because it was mentioned that below certain scale the structure was unaffected by the constrains, this fact forces to perform different additional realizations in order to get the appropriate candidate for the low scales that resembles the known Local Group, with the correct properties: two main halos similar to the Milky Way and Andromeda with corresponding masses, relative positions, velocities, etc. This was achieved by making a large number of realizations with 256^3 particles, letting the system evolve from the starting redshift $z = 50$ until the present day $z = 0$. The method of imposing the constrains for high resolution realizations, which were set up with the maximum number of available particles (4096^3) that could be allocated, was by making the FFT-transformation, into the k-space, of the desired realization and then substituting the own natural low k modes with those of the pretended k representing the observations. This way, the realization has unconstrained high k modes (low scales) and constrained low k modes (large scales).

Summing up (*Santos-Santos et al. 2015*), the large scales, greater than $\approx$

$5h^{-1}$Mpc, of the simulations (low resolution) were represented by adding the previously introduced observational data to realizations of Gaussian random fields what, computationally speaking, was achieved using the TREEPM N-body algorithm alongside SPH code of GADGET2 (*Springel 2005*). Once the large scales are set up, in order to settle the low scales, "high resolution" version for distances smaller than $\approx 5h^{-1}$Mpc were performed, to find the correct realizations showing the correct properties of the Local Group were chosen as candidates, which was achieved with another code, *Gasoline* (*Wadsley et al. 2017*), an analogous code to GADGET but with several differences that are explained in a little more detail in the next section.

Through the method explained above two kind of initial conditions were produced, the first one is low resolution oriented, that is, focused in obtaining the large scale structure of the whole simulation in a computational box o side $L = 64h^{-1}$Mpc with enough resolution to be able to distinguish individual halos that could be related to dwarf galaxies in the real universe. For this low resolution simulations only a third amount (1024) of the maximum number of particles available were used. The purpose of the second set of initial conditions was to re-simulate the Local Group candidates found in the low resolution one, to reproduce a high resolution version of them with the total number of available particles, in a region equivalent to a sphere of $2h^{-1}$Mpc centered in the Local Group. This second set of initial conditions were simulated from redshift $z = 100$ to avoid some effects of cell crossing in the high resolution volume.

2.2 Description

Two types of simulations were produced, a pure N-body run with only dark matter particles and a hydrodynamical simulation (which includes gas dynamics, star formation, stellar feedback, etc.) with both dark matter and gas particles. This high resolution region was reproduced with the latter simulation type whereas the former was used for the low resolution region (or higher particle mass), as just gravitationally driven large scale structures are looked for.

There are two sets of cosmological parameters for these simulations, WMAP3 and WMAP5, although the latter set was not implemented in the high resolution run. The parameters of this set are $\Omega_m = 0.24$, $\Omega_b = 0.042$, $\Omega_\Lambda = 0.76$, a normalization value of $\sigma_8 = 0.73$ and a slope for the power spectrum of $n = 0.95$.

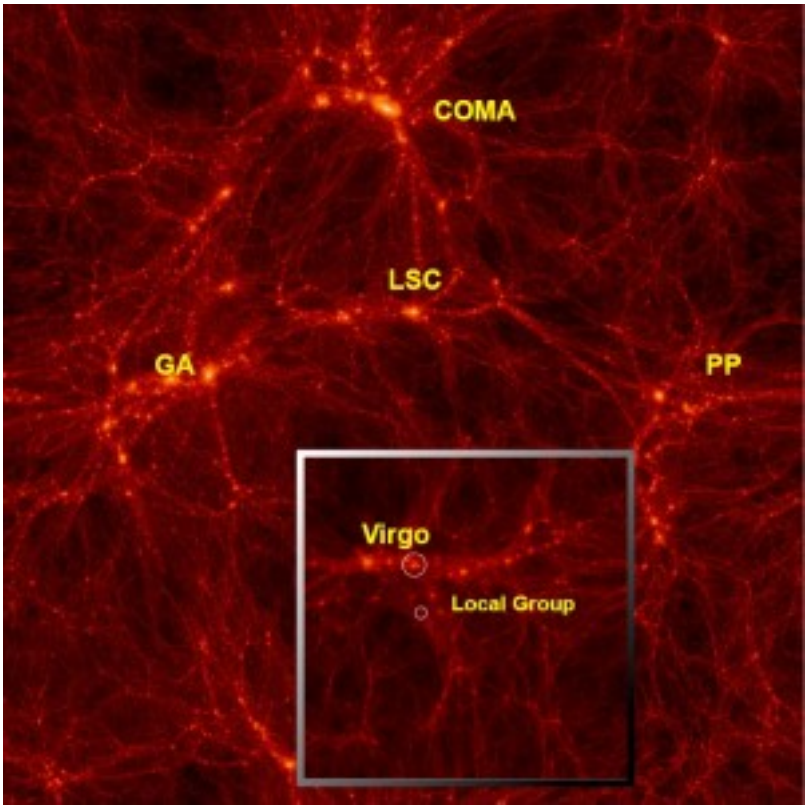

Figure 2.1: Illustration of the dark matter distribution of the Local Universe in the simple N-body run. *https://www.clues-project.org/cms/*

2.2.1 Dark Matter

As previously said, under the ΛCDM model, the dark matter prescription assumed is the so called *Cold Dark Matter* where the dark matter particles are assigned a mass of $m_{DM} = 2.95 \cdot 10^5 h^{-1} M_\odot$ has been established for the high resolution run, being the mass higher for the low resolution one.

Focusing on the low resolution simulation, in figure 2.1 it is shown the dark matter distribution and structure of the vicinity of the Local Group, in a box of $160h^{-1}$ Mpc side length, with a smaller box of $64h^{-1}$ Mpc side length zooming in into the Local Group candidate, in the LSC (Local Super Cluster) area. Due to the observations, not only the cosmic web can be clearly seen (alongside with the dark matter filaments and clusters) but also being able to identify the neighbouring clusters as the Coma cluster or the Great Attractor, as examples.

2.2.2 Hydrodynamics

Once an acceptable analogue of the Local Group has been found in the Local environmental simulation (the pure N-body run with GADGET2 code from $z = 50$ to $z = 0$), a second run is performed, a high resolution re-simulation (using *Gasoline* code) with the maximum resolution available (4096^3 particles) that contains not only dark matter but a complete set of hydrodynamical physics where the particle resolution is (*Santos-Santos et al. 2015*): $m_\star = 1.3 \cdot 10^4\ M_\odot$, $m_{gas} = 1.8 \cdot 10^4\ M_\odot$ and $m_{dm} = 2.9 \cdot 10^5\ M_\odot$, with softening lengths of $\epsilon_{bar} = 223$ pc between baryons and $\epsilon_{dm} = 486$ pc between dark matter particles.

As baryon particles are included in the high resolution run, hydrodynamical physics must be taken into account, processes that are encoded in the previously mentioned *Gasoline* code, which have different prescriptions for star formation, cooling , feedback, etc.

Giving an overall look on the hydrodynamics, being all the events named instantaneous: the interstellar medium (ISM) is set as a medium composed of hot gas and cold gas clouds in pressure equilibrium, whose properties and evolution are shaped by the energy and metals released by the stars. The energy released by supernova explosions is implemented as a "blast-wave" into the ISM, accounting for each release an amount of energy of $\epsilon_{SN} x 10^{51}$ erg is delivered.

In the *Gasoline* code (*Governato et al. 2010*), the cooling origin is radiative, where the ionization and excitation states of the gas particles are modelled by the features of a uniform background radiation field and its strength. The background radiation field used, the cosmic ultraviolet background, is implemented using the Haardt-Madau (*Haardt and Madau 1996*) model, including photoionizing and photoheating events produced by population III stars, "Quasi-Stellar-Objects" and galaxies starting at $z = 9$. All these cooling phenomenon are performed in a primordial mixture of hydrogen and helium at high temperatures, including the effects of metal cooling and evolving gas metallicities below 10^4 K.

The feedback is proposed as kinetically driven, ruled by winds coming from supernova explosions, feedback that in the end can be tweaked by the cooling rate established. The amount of supernova events that are produced is determined stochastically, setting that a fraction of the stars will end their lives as a supernova. The chances for the target particles to receive this feedback is given by a certain probability that depends merely on being near a star forming area, who are more likely to receive those winds (dependent of the star formation rate and the total amount of energy release). Following this topic of the formation of stars, a recipe

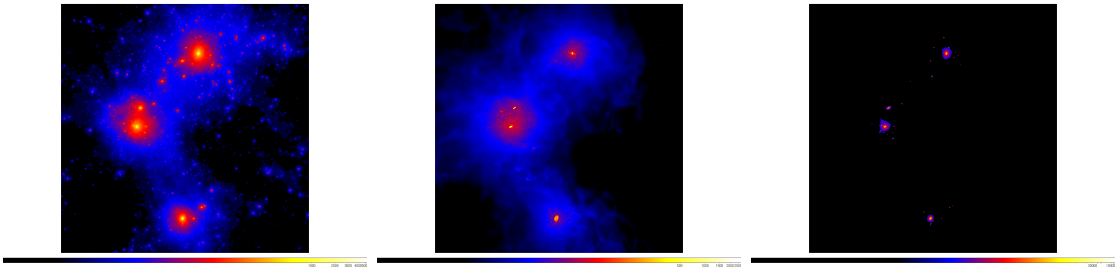

(a) Dark matter content **(b)** Gas content **(c)** Star content

Figure 2.2: Distribution of dark matter (*left panel*), gas (*middle panel*) and star (*right panel*) particles of the high resolution re-simulation of a Local Group candidate. *https://www.clues-project.org/cms/*

for the star formation based on the Schmidt law is implemented: once the gas particles get colder and denser, stars start forming with a star formation rate of $\propto \rho^{1.5}$.

Regarding the high resolution re-simulation, in figure 2.2 are shown the images, all of them represented in a box of $1.3h^{-1}$Mpc of side length, of the individual distributions corresponding to each of the three types of matter present in the simulation (dark matter, gas and stellar particles), with all the main galaxies clearly visible, which are, from top to bottom: the Milky Way, Andromeda and Triangulum Galaxy (M33).

Summarizing, there are two types of simulation, one is a pure N-body simulation with only dark matter particles for the low resolution run whose aim is to reproduce the large scale structure of the Local Universe. Once the large scales are settled, the second type arises, a high resolution re-simulation for the most suitable Local group candidate.

Chapter 3

Methodology

3.1 Sample Selection

In this section, we comment in more detail the considerations that have been made and tools and procedures followed to obtain and analyze the results, which are shown in the next section.

Our target galaxies are selected, at the present time $z = 0$, as those that fulfill the following properties:

- The selected group of galaxies are classified as dwarfs, what means that they are not any of the two main halos of the Local Group (neither Milky Way nor Andromeda).

- Thay need to have at least 50 stars, as a simulated galaxy with fewer stars can be difficult to study.

- They need to be isolated, which means that their position in the present time, $z = 0$, is outside of the virial radius of the two main halos, that does not imply that they could not have been inside the virial radius of a more massive halo in the past. This property helps to assume that the target galaxy was not absorbed by a bigger halo or being stripped of their gas and quenched, etc. This enables the chance to believe that the past of the galaxy (birthplace and evolutionary path) still have their impression on the present properties.

- They can be considered as part of the Local Group, which means that the distance of each dwarf galaxy to either the Milky Way or Andromeda is not greater than ≈ 2 Mpc, this limit is set by this work to ensure that all the galaxies inside

this limit are members of the Local Group.

The selected group of galaxies appear in little more detail in table 3.1, in it the chosen galaxies are mentioned alongside some relevant data. The mentioned classification into *fast* or *slow* dwarfs, as was introduced in the first section, according to the definition of the combined work of *Gallart et al. 2015* and *Bermejo-Climent et al. 2018*. If one galaxy formed the 50% of the stars before $z = 2$ it will be set as a *fast* type, otherwise, it will be considered a *slow* type.

ID	Type	$t_{50\%}$ (Gyr)	M_T at $z = 0$ $(M_\odot)$	$M_\star$ at $z = 0$ $(M_\odot)$
2	Fast	3.4	2.66E+11	5.08E+09
16	Fast	3.0	1.21E+11	1.57E+09
18	Fast	2.8	8.01E+10	1.10E+09
20	Slow	5.8	6.54E+10	3.78E+08
21	Slow	4.2	3.87E+10	5.40E+08
24	Slow	4.0	4.05E+10	3.30E+08
30	Fast	3.0	3.37E+10	2.10E+08
44	Slow	6.4	2.92E+10	6.21E+07
49	Slow	4.2	2.40E+10	2.02E+08
50	Slow	6.8	2.34E+10	2.57E+08
51	Slow	5.2	2.39E+10	9.57E+07
52	Slow	8.4	2.23E+10	1.26E+08
58	Fast	2.2	1.68E+10	6.92E+07
61	Slow	4.0	1.36E+10	2.38E+08
64	Fast	2.8	1.57E+10	4.53E+07
65	Slow	5.6	1.39E+10	1.51E+07
66	Fast	3.0	1.50E+10	3.92E+07
75	Slow	5.8	1.31E+10	2.04E+07
89	Slow	10.8	1.06E+10	5.93E+06
95	Slow	5.0	9.61E+09	7.75E+06
98	Slow	7.4	8.62E+09	2.33E+07
100	Slow	4.0	8.99E+09	2.07E+07
101	Slow	10.2	8.44E+09	2.01E+07
120	Slow	5.4	6.70E+09	9.40E+06
125	Fast	3.2	6.91E+09	7.12E+06
126	Slow	5.4	6.79E+09	6.48E+06
129	Slow	6.2	6.50E+09	5.93E+06
154	Slow	5.8	5.51E+09	3.75E+06
156	Slow	5.0	5.13E+09	2.45E+06
166	Fast	1.8	4.73E+09	1.26E+07
168	Slow	9.4	4.71E+09	2.12E+06

173	Slow	6.4	4.46E+09	9.85E+06
176	Slow	4.0	3.74E+09	4.18E+07
190	Fast	3.2	3.92E+09	1.28E+07
278	Fast	3.6	2.41E+09	1.01E+07
294	Slow	8.6	2.33E+09	2.19E+06
298	Fast	3.4	2.25E+09	4.08E+06
315	Slow	4.0	2.10E+09	9.64E+06
328	Fast	3.6	2.03E+09	3.12E+06
335	Fast	2.6	2.05E+09	3.46E+06
355	Fast	2.2	1.92E+09	1.15E+06
387	Fast	2.4	1.61E+09	5.78E+06
542	Fast	1.6	1.04E+09	9.09E+06

Table 3.1: The selected target galaxies represented by some important features apart from a simple identification number: the type, the time relevant to the classification in fast or slow, the total mass of the galaxy at $z = 0$ and the total stellar mass at $z = 0$.

In figures 3.1 and 3.2, some examples of this method of galaxy classification can be appreciated. In the former figure, being both galaxies *fast dwarfs*, where can be seen that, although they have kept an almost residual star formation rate until present time, they formed a significant amount of their stars (a 50% threshold is considered) by $z = 2$ It can be worthwhile to point out that, although the SFH of the left panel in figure 3.1 shows a not negligible star formation rate between $z = 2$ and $z = 1$, this fact can mislead to the thought that this galaxy may be a *slow* type dwarf. However, a deeper but easy analysis can proof that, for that galaxy

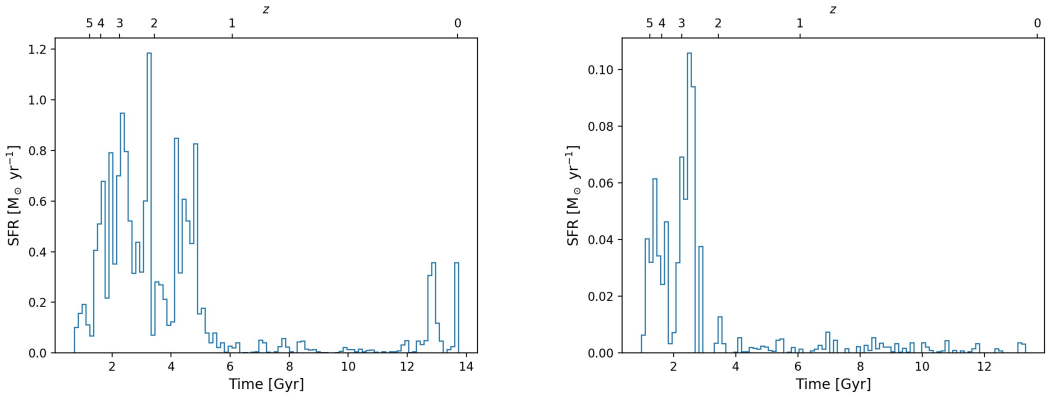

Figure 3.1: The star formation history of two *fast dwarf* type galaxies.

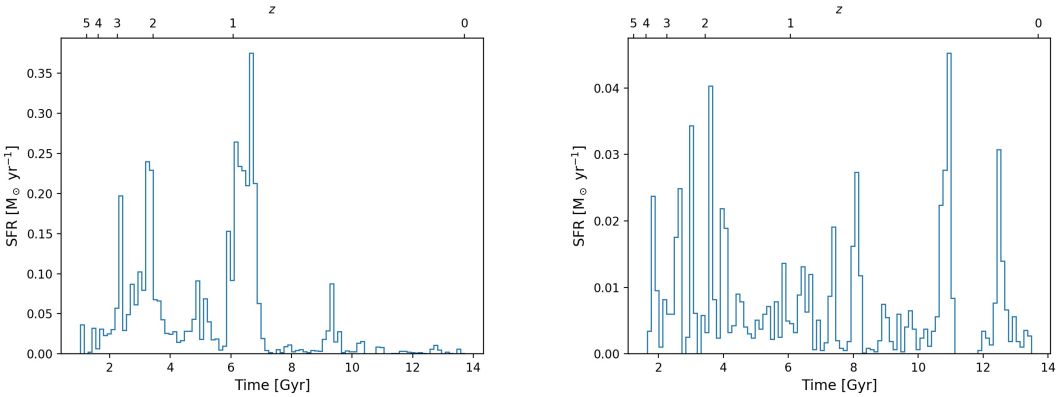

Figure 3.2: The star formation history of a couple of *slow dwarf* type galaxies.

at $z = 2$, more than half of its total amount of stars at the present were formed. Continuing with the later figure, it shows the counter part, a couple of *slow dwarf* galaxies that either they have had, on average, the same star formation rate over their whole lifetime (a star formation period that lasted until the present time) or they formed the majority of their stars after $z = 2$ (the main star formation period already ended).

3.2 Observational Data

Despite the theoretical approach, made in this work, to the problem presented in the previous sections, whatever are the found results must be in good agreement with the observations in order to be proven and tested, as they establish the hypothesis that may be correct. In our case, as the source of data is a simulation (as constrained by the observations as it may be, it still is a simulation), at least a confirmation is needed that the galaxies obtained by it, and its properties, resembles the ones that are observed in the universe.

Focusing on the observational "checking" of this work, we use some results present in *Bermejo-Climent et al. 2018*, where they compare some properties (as, for example, the present day stellar mass and the dynamical mass at redshift $z = 0$) of 16 measured galaxies (well known before the SDSS) in the Local Group, 15 of those were also used in *Gallart et al. 2015*, excluding the Large Magellanic Cloud, Small Magellanic Cloud, and IC1613. The purpose of this comparison is worthwhile to explore how close are the mentioned properties of the observed galaxies with the analogous of our simulated dwarfs.

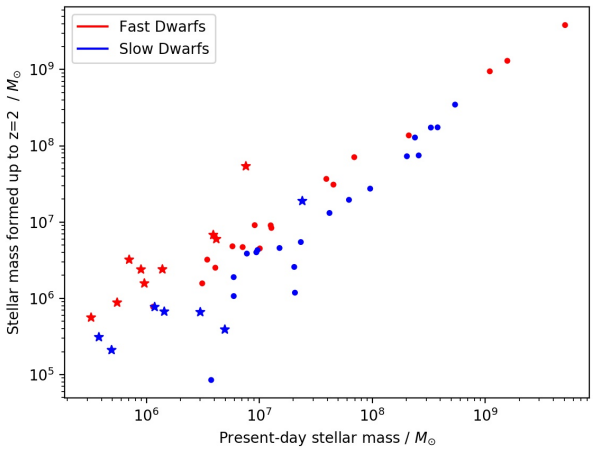

Figure 3.3: Comparison between the stellar mass formed up to $z = 2$ vs the present day stellar mass. The stars represent the observations (*Bermejo-Climent et al. 2018*) and the dots the simulated galaxies.

In figures 3.3 and 3.4 this comparison is presented, where the are superposed the plot with the observations alongside the equivalent one with our data, equivalent because one magnitude was not be obtained with the same method, the procedure followed in that case is explained below. The galaxies of the original work are shown as stars and the galaxies from this work as circles, in addition, we add the classification method of *fast dwarfs* and *slow dwarfs* in these plots, representing the former by red color and the latter in blue color (both cases despite of the marker used).

One important difference is that the dynamical mass, in the observations, was calculated via equation 3.1 using measurements of the half-light radius of the galaxies and their velocity dispersion. For our case, we compute this quantity by summing all the matter content inside a sphere of radius equal to the half-light radius.

$$M_{dyn} = 580 \cdot r_{half-light} \cdot {\sigma_v}^2 \tag{3.1}$$

All the three plots show that our data is, in general, in good agreement with the observations, in a sense that the simulated galaxies have properties compatible

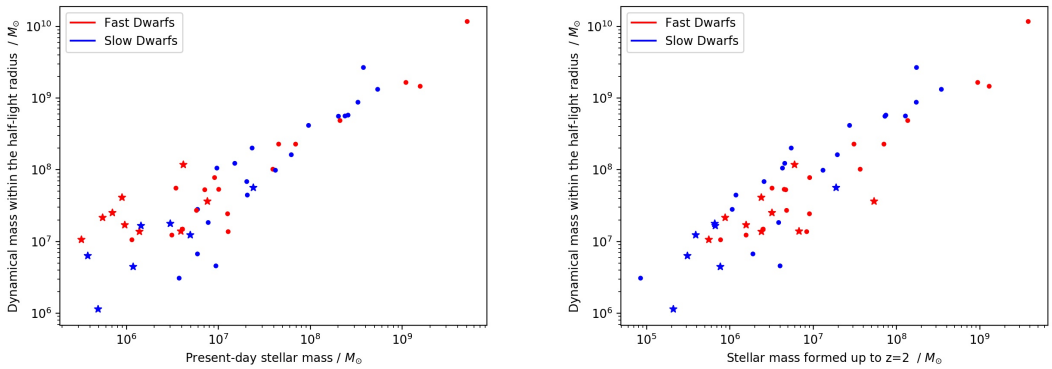

Figure 3.4: Comparison between the dynamical mass at $z = 0$ vs the total stellar mass at $z = 0$ and at $z = 2$, *left panel* and *right panel* respectively. The same way as figure 3.3, the stars represent the observations (*Bermejo-Climent et al. 2018*) and the dots the simulated galaxies.

with the ones that are observed in the galaxies of the real Local Group. Agreement that in the end allows us to claim that the findings made are plausible to be the solution to the discrepancies studied.

3.3 Time Analysis

As mentioned previously, along with the purpose of this project, we seek to know the properties in the past of the place and environment where galaxies where formed, for that reason, here we present the main tool that helped us finding each galaxy between many snapshots of the simulation. At this point we can introduce that, the mentioned "environment", will be settled between 1 and 5 times the virial radius of each galaxy.

The *bridge* module, which is part of the main software used for the whole analysis of the results, is the primary tool used in the connection of two snapshots of the simulation. When two timesteps are about to be linked, the procedure this module uses is search an "id" assigned to each particle in both steps, when a certain number of "ids" have been found (depending on the threshold settled), the module establishes that the corresponding halo, and galaxy, has been found. This means that a minimum number of particles are needed in order to successfully match a halo in the new snapshots.

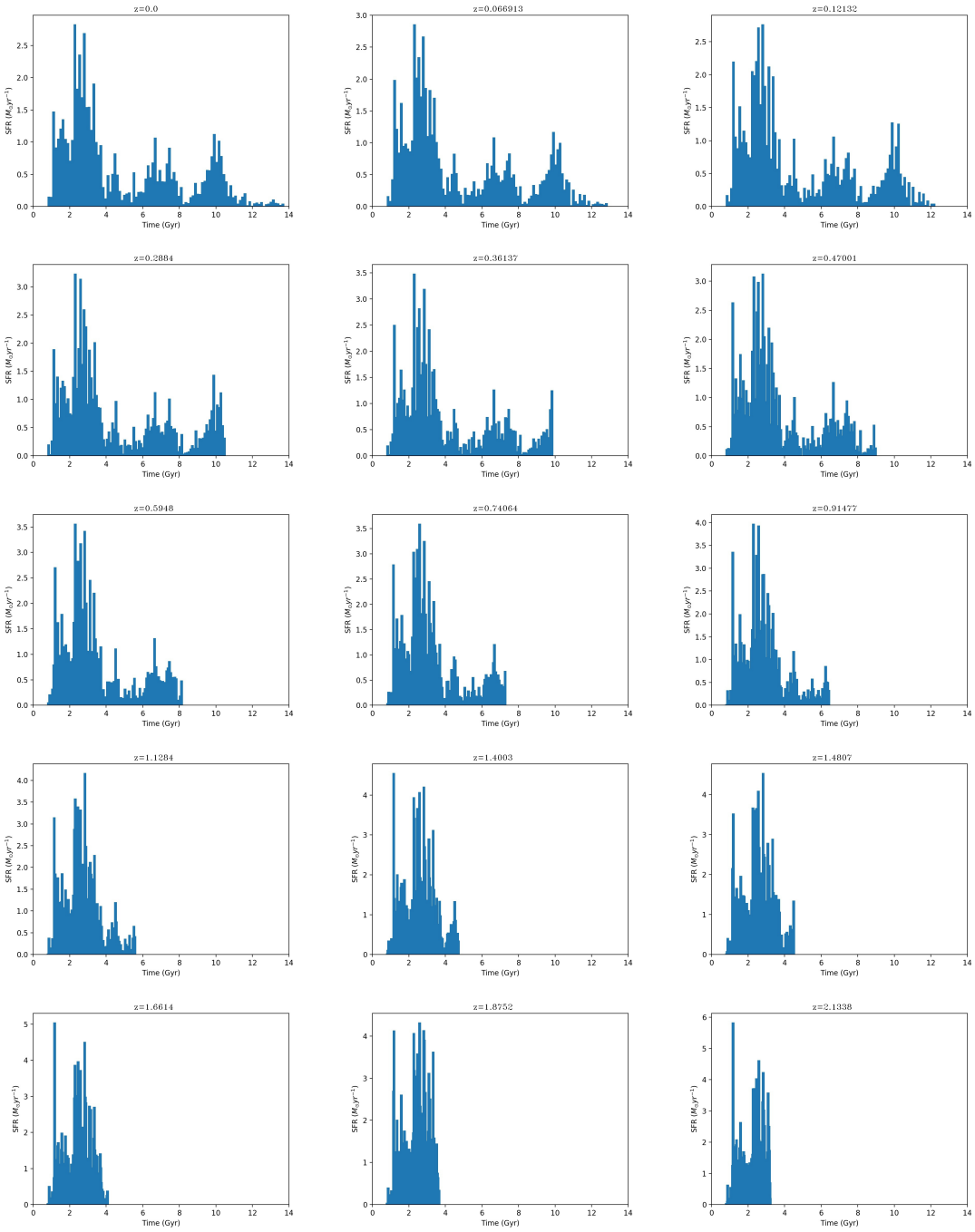

Figure 3.5: An example of tracking a single dwarf galaxy, via star formation history, across several redshifts, with increasing lookback time from *top left* panel to *bottom right* panel.

In figure 3.5 there are a series of the star formation history of one galaxy, serving as a test sample, to check how a galaxy can be found in other timesteps rather than the present time. *Top left* plot represents the starting point at $z = 0$, for the rest of the plots, the bridge module was used to locate the "probable" new halo, then its star formation history was plotted and checked with the known one of the previous snapshot, this allows us to see if it is plausible that the halo suggested by the bridge module is the correct one. In the series of plots can be seen that, in general, the star formation history is the same one (in terms of the shape of it) but shortened as we travel to higher redshifts, what indicates that the bridge module is working perfectly, for that galaxy, and the represented galaxy was correctly found in other snapshots. In addition, in the appendix there are the star formation histories at $z = 0$ of the rest of the sample group.

Unfortunately, nothing is never as easy as the theory (or the initial tests) might suggest because, as mentioned, this bridge modules algorithm uses, at least partly, the "ids" given to the stars to look for them in the new timestep and assign the new position according to the halo where those "ids" were found. In practice, what this finding method really means is that any interaction the galaxy might have had, that could have stripped stars from itself, is going to make harder (maybe even impossible) the work of this tracking module because not only the id would not be found where they were suppose to be but perhaps the number of particles (or their positions) is not enough to assure that the chosen galaxy is the one that was searched. For this reason, several test needed to be run (as the previously mentioned star formation consistency) to be sure that the traced galaxy was the chosen one.

The main focus of the analysis of each galaxy can be resumed in the following arguments:

- Studying the variation on the total mass of the galaxies over the time which means, in other words, to check how much the mass of the stars formed changed the mass of the galaxy a throughout their lifetimes, information that can complement with the star formation history plots.

- Obtaining the individual environmental density (between 1 and 5 virial radius of each galaxy) in some representative redshifts and compare it with the rest of the galaxies.

The goal of the first argument is to check the kind of total mass growth did each galaxy have, considering its type (either *fast* or *slow*), from around $z = 2$ to the present day at $z = 0$. As it was said several times, the star formation history at

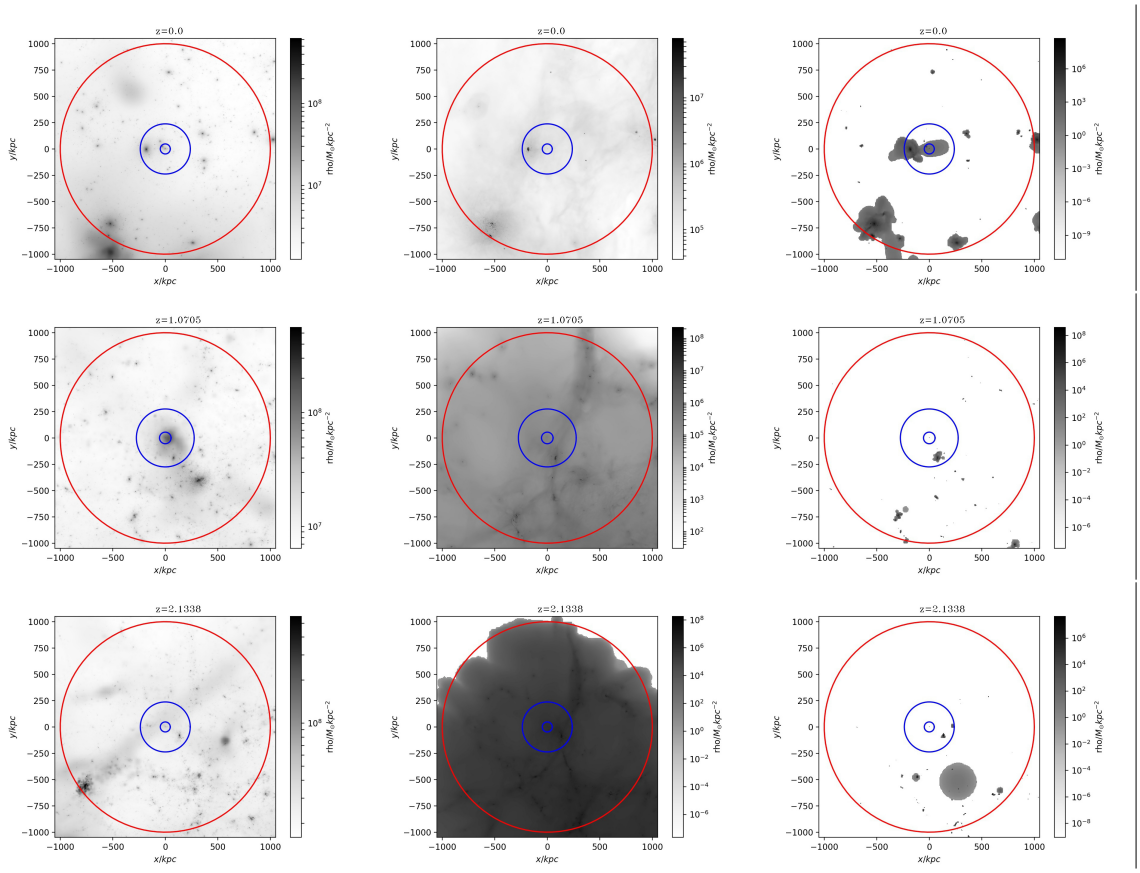

Figure 3.6: Images of dark matter (left column), gas (middle column) and stars (right column) for a *fast* galaxy at $z = 0$ (first row), $z \approx 1$ (second row) and $z \approx 2$ (third row).

$z = 2$ settles the difference between a *fast* type and a *slow* type dwarf, so exploiting this feature it can be studied if, for example, a *fast* type galaxy has had a quicker mass accretion history around $z = 2$, what translates in an earlier big total mass increase as it is suppose to be born in an environment with higher density (from the average). Compared to a *slow* type dwarf, which could have had its major mass accretion period at later times because of the opposite reasoning given to the *fast* type one, that is, at $z = 2$ the overdensity was not strong enough and the star formation was not altered.

The second argument, on the other hand, serves to check the environment in which dwarf galaxies were formed and the possibility that it affected the star formation of the galaxy, the reason is because it could happen that a fast dwarf

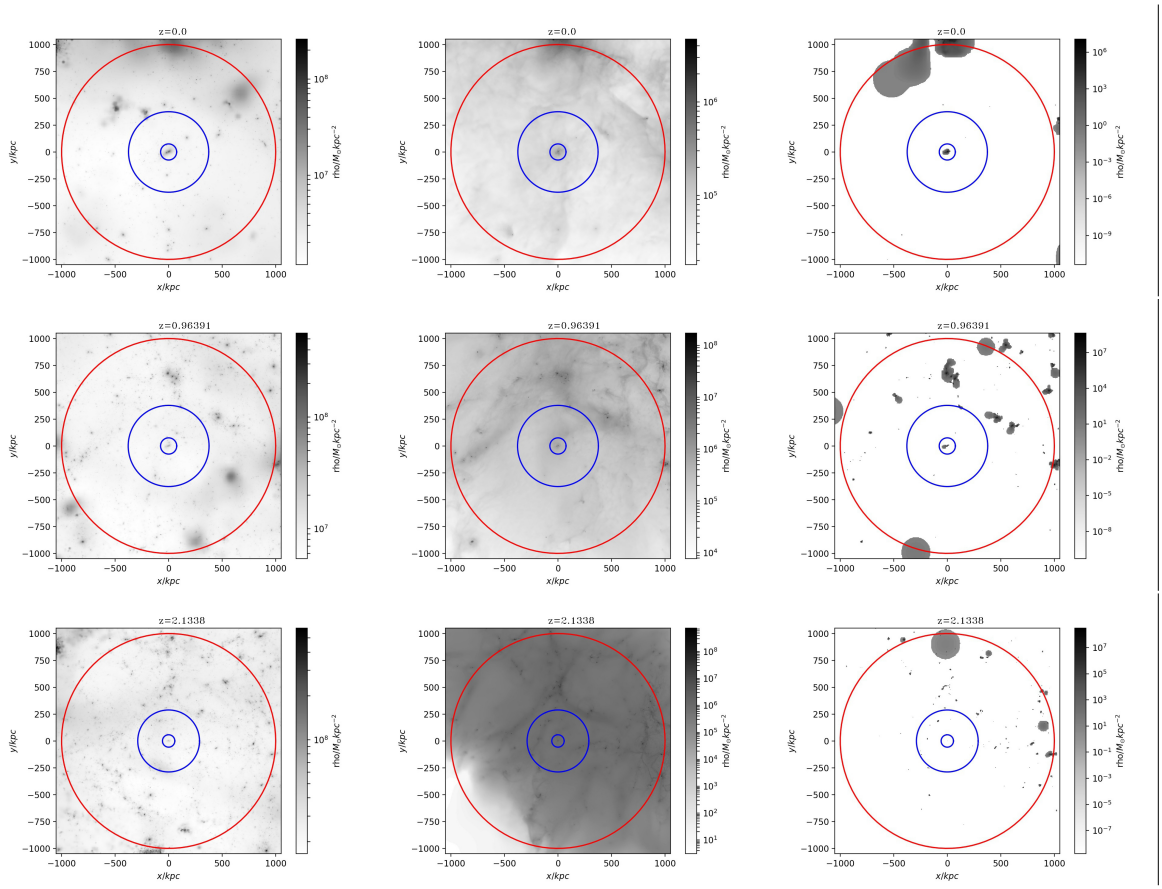

Figure 3.7: Same images of matter content but for a *slow* type galaxy at, roughly, the same redshifts as in figure 3.6.

suffered some kind of interaction that "cleaned" its neighbourhood and affect its star formation eventually and the growth curve of the total mass. As a helping resource for visual interpretation, we use images of dark matter, gas and stars for every galaxy and every timestep studied (centered in the target galaxy, of course), not just to try to look for the overdensities in the density plot with the environmental images but to check the tracking consistency. A couple of examples of these matter images are shown in figures 3.6 and 3.7, where images for the mentioned three types of matter are represented for a fast (former figure) and a slow galaxy (latter figure) in some particular redshifts of our analysis.

In addition, the area enclosed by red circles in the images represents a sphere of radius of 1 Mpc around the galaxy whereas the blue circles represent the area between 1 (inner blue circle) and 5 (outer blue circle) virial radius of that galaxy.

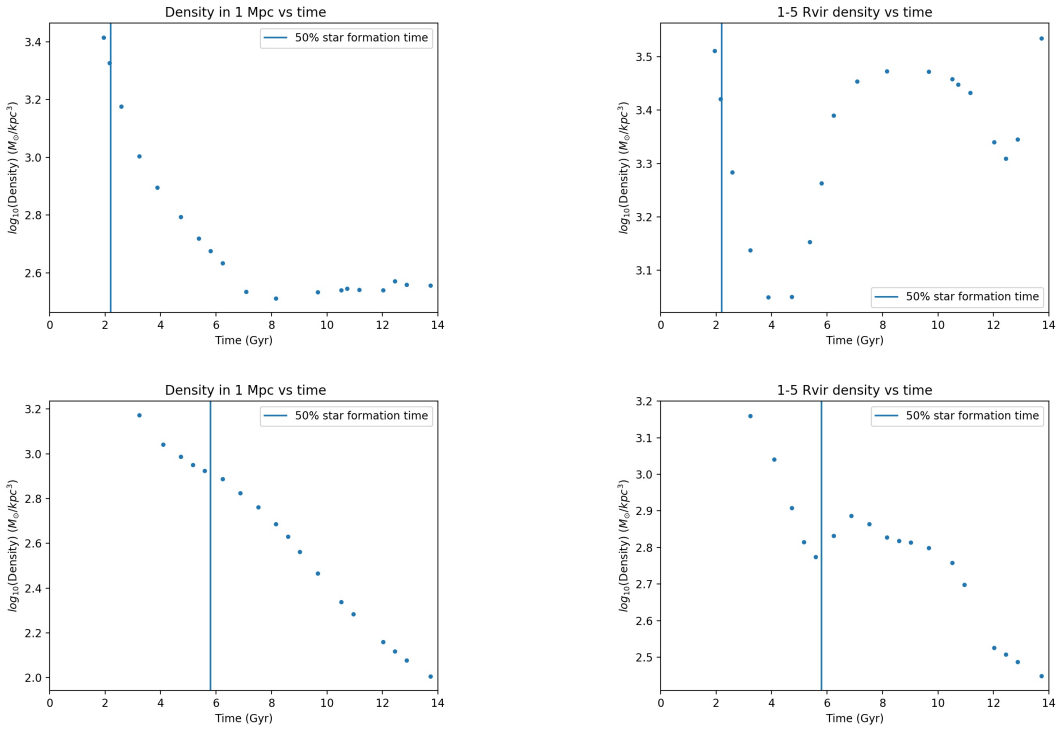

Figure 3.8: The evolution of the environmental density for a *fast* dwarf (first row) and a *slow* dwarf (second row). Each blue vertical line represent the time when that galaxy formed the 50% of the stars.

These distances were set up to be able to keep a somehow control on how the environmental density, inside those areas, of the galaxies was evolving over time, this way the analysis could be ease up and more complete. In that regard, in figure 3.8 it is shown the representation of the evolution of the mentioned densities, corresponding to the area of a sphere of radius of 1 Mpc (left column) and the area between 1 and 5 virial radius inside the blue circles (right column) for the same specific couple of galaxies. As was the case for the star formation history ones, the plots of these environmental density for the rest of the galaxy sample are in the second part of the appendix.

Chapter 4

Results

In this chapter we present all the most representative results of this work, focusing on the purpose of this work and the features that were previously introduced. We comment briefly our findings, saving the main discussion and their implications for the next and last chapter. Firstly it should be mentioned that, as many timesteps have been studied, we focus our results and findings in some representative redshifts: $z = 0$, $z = 0.5$, $z = 1$ and $z = 2$.

Combining, for each galaxy, the information available from its star formation history plus the evolution in time of the environmental density and adding the matter content images (that can serve as a complement for the analysis and the conclusions) almost all the necessary data sources are covered, as the most relevant

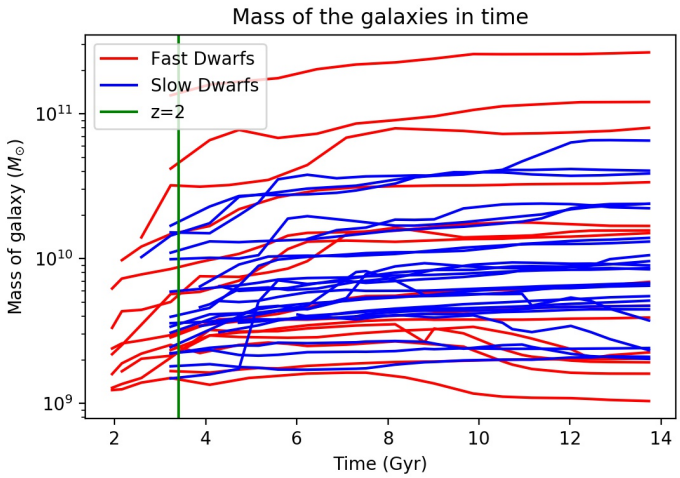

Figure 4.1: Mass accretion rates of all the studied galaxies.

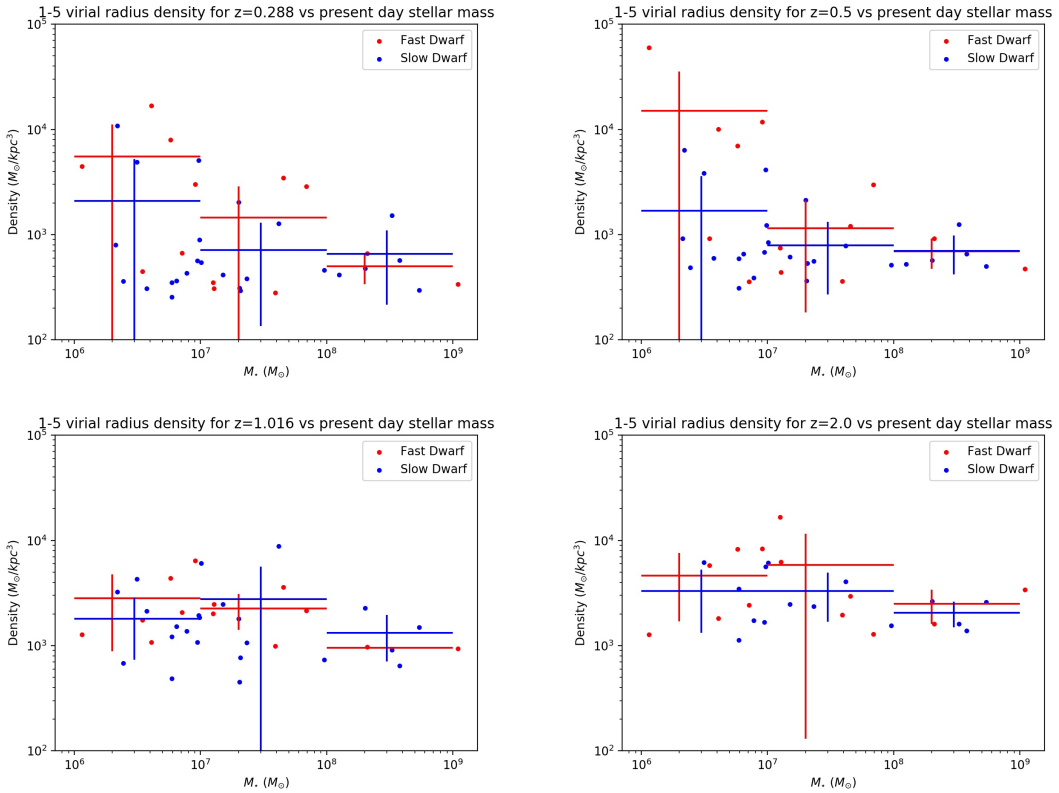

Figure 4.2: Relation of the density between 1 and 5 virial radius against the galaxies total stellar mass at the present, at different redshifts: $z = 0.288$ (top left panel), $z = 0.5$ (top right panel), $z = 1.016$ (bottom left panel), $z = 2.0$ (bottom right panel). Alongside averages (with the corresponding errors), as horizontal lines, per mass interval.

information is encoded in them and, also, because their agreement towards the galaxy they represent can be tested comparing the results given by its data resource. To highlight an example of this claim, if for example a strange mass decrease is detected for a galaxy, thanks to the density plots, of both kind, and the matter content images it may be possible to discover the reason behind that decrease and help finding an explanation to it.

Another source of information for studying the effects of the environmental activity on a galaxy, is the evolution of the total mass of the galaxy (or the mass accretion rate of the galaxy). For this reason, we change the spotlight to figure 4.1, where are represented the mass accretion rates of the galaxies of our sample, with the *fast* dwarfs represented with red lines, the *slow* dwarfs with blue lines and, in

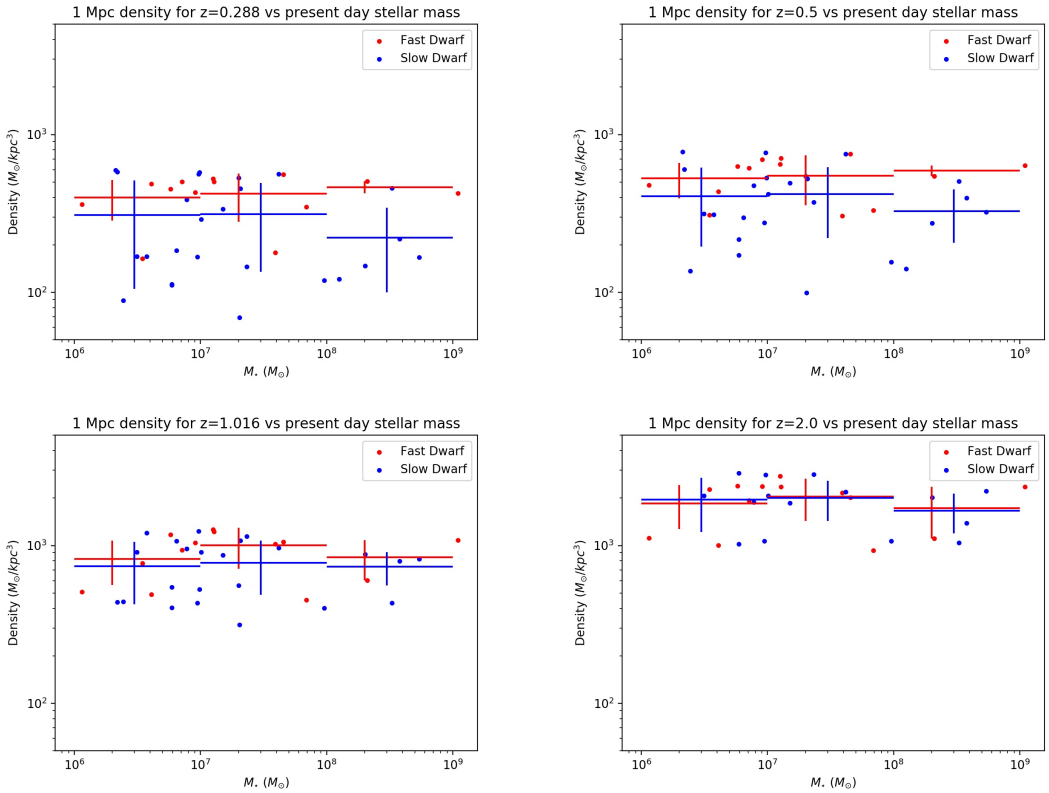

Figure 4.3: Relation of the density inside a sphere of 1 Mpc of radius against the galaxies total stellar mass at the present, at different redshifts: $z = 0.288$ (top left panel), $z = 0.5$ (top right panel), $z = 1.016$ (bottom left panel), $z = 2.0$ (bottom right panel). Alongside averages (with the corresponding errors), as horizontal lines, per mass interval.

addition, a vertical green line at the time corresponding to $z = 2$, which represents the time we use to discriminate between fast and slow dwarfs based on the fraction of stars formed up to that point. The reason to focus in this magnitude is to check if galaxies born in denser areas started earlier accreting mass.

In this latter figure, it can be appreciated that a great number of fast dwarfs experienced a considerable, and determinant at the same time, mass growth previous to $z = 2$ (although they obviously keep growing in mass after that time). However, in the case of the slow type galaxies, for all of them, it can be seen that the major growth in mass happened after $z = 2$ (in some cases very after that time). In general, the time interval between 5 and 9 Gyr may be the most representative times for that main growth of the slow types.

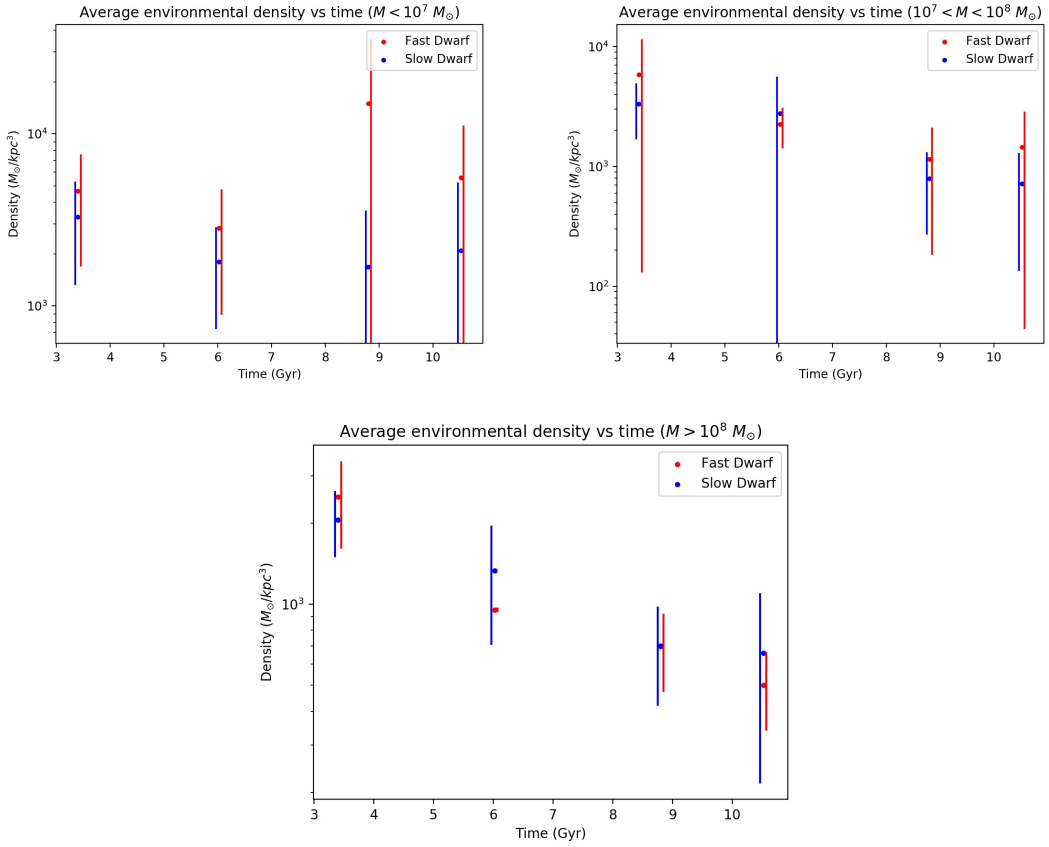

Figure 4.4: Environmental density between 1 and 5 virial radius in the times representing $z = 0.28$, $z = 0.5$, $z = 1.016$ and $z = 2.0$ for mass intervals of $< 10^7$ $M_\odot$ (*top left* figure), $10^7 < M < 10^8$ $M_\odot$ (*top right* figure) and $> 10^8$ $M_\odot$ (*bottom* figure), with an error of 1σ.

Another data resource is represented in figures 4.2 and 4.3, there it is shown the density between 1 and 5 virial radius (in the former figure) and inside a sphere of 1Mpc (for the latter one) of each galaxy versus the total stellar mass each one has at the present time $z = 0$, for several redshifts, $z = 0.288$, $z = 0.5$,$z = 1.016$ and $z = 2.0$. In addition, three mass intervals were established to study the plots: $M < 10^7$ $M_\odot$, $10^7 < M < 10^8$ $M_\odot$ and $M > 10^8$ $M_\odot$, alongside the average densities, as horizontal lines, in each interval for fast galaxies and slow galaxies, each one with its error bar (the error being one standard deviation).

In these plots, including 4.4, several features could be studied, for example, at all redshifts (in general) the fast type galaxies are living in denser environments,

at all mass intervals, with respect to the slow type ones, specially are the least massive galaxies (the ones with masses under 10^7 $M_\odot$) the group that fulfill the assumption made more notably. However, this is a suggestive result and be taken with caution as all the cases are within a 1σ error. Even so, this result is promising on the idea that, as it was the same period of time when most of their stars were being formed, a denser environment for those galaxies is a plausible explanation. At this point, a useful and important argument is that it would not be shocking to assume that denser environments imply faster gas accretion rates. The reason behind the general density drop seen as we get close to $z = 0$ is because the the newly formed structures (galaxies, clusters, etc.) in time group together and cluster into bigger groups, filaments, etc. producing a progressive density drop that clean up their environment, it is true though that this effect starts to be notorious at scales around and 1 Mpc and beyond.

Another fact to look at can be that, in the period when the slow type galaxies had their main star forming epoch (roughly between $z = 1.016$ and $z = 0.5$), a main feature can be highlighted. In the transition from $z = 2.0$ to $z = 1.016$ all the slow dwarfs, speaking in terms of averages, experienced a very slightly density drop, as their main star formation era was yet to come, while the density of the fast dwarfs decreased (in the case of two out of three mass intervals even surpassing the average fast type density). Adding this situation to a slower star formation rates for the slow type galaxies, as they are in general in less dense environments, could be linked to the fact that slow type galaxies experienced their main star formation time from around 6 Gyr ($z = 1.016$) to almost 9 Gyr ($z = 0.5$) when these galaxies suffered the environmental density drop, as the mentioned slower star formation rate provoked the delay of the formation of the stars compared to the one of the fast type galaxies.

It can be worthwhile to point out that, almost as a curious fact, in the most recent plots (close to $z = 0$) low mass galaxies, specially fast types, had a great environmental density from where one might think that it could imply a new star forming period, instead, from figure 4.1 can be seen that the low mass galaxies (including both types) if the mass do not remained constant it decreases. An explanation to this can be that, as they are low mass galaxies, it is not unlikely that they could be more vulnerable to be swallowed by other more massive halos or at least be affected by them, for example getting their gas stripped away. Effect that could be added to the fact that a significant number of stars ended their lives, warming up the surrounding gas and preventing new stars from being formed, preventing more stars from being formed.

Chapter 5

Summary & Conclusions

The aim of this work is to shed light to the hypothesis emerged combining the works of *Gallart et al. 2015* and *Bermejo-Climent et al. 2018*, this hypothesis stands that the difference in the star formation history between the so-called fast and slow type galaxies (understanding by *fast* and *slow* types those who formed the 50% of their stars before and after $z = 2$, respectively) may be explained by an initial environmental overdensity in the case of the fast galaxies (respect to the slow type ones), compared to the one that slow galaxies may have had, that could explain the reason these galaxies had a faster and more intense star formation rate than their slow type companions. To be able to work on this hypothesis, we use a set of simulations called CLUES (*Gottloeber et al. 2010*) which is a set of cosmological hydrodynamical simulations whose aim is to reproduce the observed data of the Local Universe, constraining the parameters that represent the known scales by the observations.

Firstly, our galaxy sample needed to be prepared, for that reason, we selection criteria was based on a couple of essential conditions: being isolated (outside the virial radius of the most massive halos of the Local Group) at $z = 0$ and having at least 50 stars, the resulting sample group consist of 40 galaxies, being 15 fast type and 25 slow type, out of around 350 galaxies available in the whole simulation. The mentioned classification into fast or slow was made studying the star formation history of each galaxy, and checking whether the time where the 50% of their stars were formed was before or after $z = 2$, being a fast type in the former case and slow type in the latter. The mentioned criteria for choosing our galaxy sample is based on the need of the agreement of our results with observed galaxies, comparison that was made thanks to the work of *Bermejo-Climent et al. 2018* in figures 3.3 and 3.4, comparing the present day stellar mass with the stellar mass formed up to $z = 2$ and with the dynamical mass, as this agreement enable us to treat our sample as if they were observed rather than simulated.

Secondly, the method we use to study each galaxy in time is through the bridge module of our software package pynbody. The essentials about this module is that it tracks down halos looking for the ids given to the particles in other timesteps of the simulation, an example of how we can be sure that we are studying the correct galaxy is shown in figures 3.5 (cheking the star formation consistency) and 3.6 (via the matter and the environment). Using these cheking tools we can be moderately sure that the results of this work may have the necessary accuracy to represent the histories of the galaxies in the real universe.

Finally, changing the spotlight to the analysis of the data, first we can appreciate that the mass accretion histories of the galaxies (figure 4.1) show that the main star formation period of the fast type galaxies occurred, in general, before than for the slow type ones. Attempting to give explanation to this difference, focusing on the environmental densities and their averages (figures 4.2 and 4.3), it is plausible to say that, in general, the variations (specially the decreases) in the average density can be correlated to the main star formation epochs of the galaxies. Overall, it can be said that in general fast type galaxies live in high density environments for all the mass intervals studied, but this conclusion must be taken with caution as the difference between the fast and the slow types are inside an error of 1σ, being also true that the least massive galaxies are the ones follow better the relation *fast type <-> high density environment*. Although it can be true that a tendency is visible and the hypothesis made may be correct, for future works a much larger sample of simulated galaxies should be used in order to get a better statistical significance.

Appendix A

Extra data

Firstly, we present the star formation histories of the rest of the galaxies:

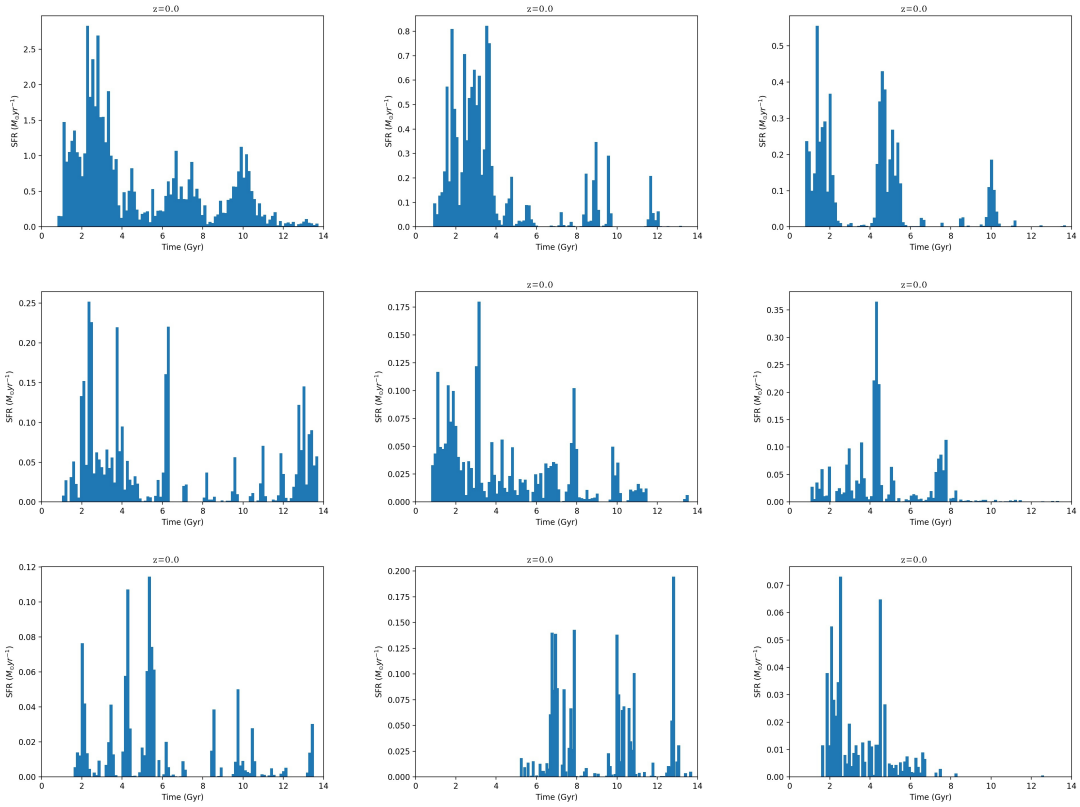

Secondly, we show the plots of the density in a sphere of 1 Mpc and between 1 and 5 virial radius for the rest of the galaxy:

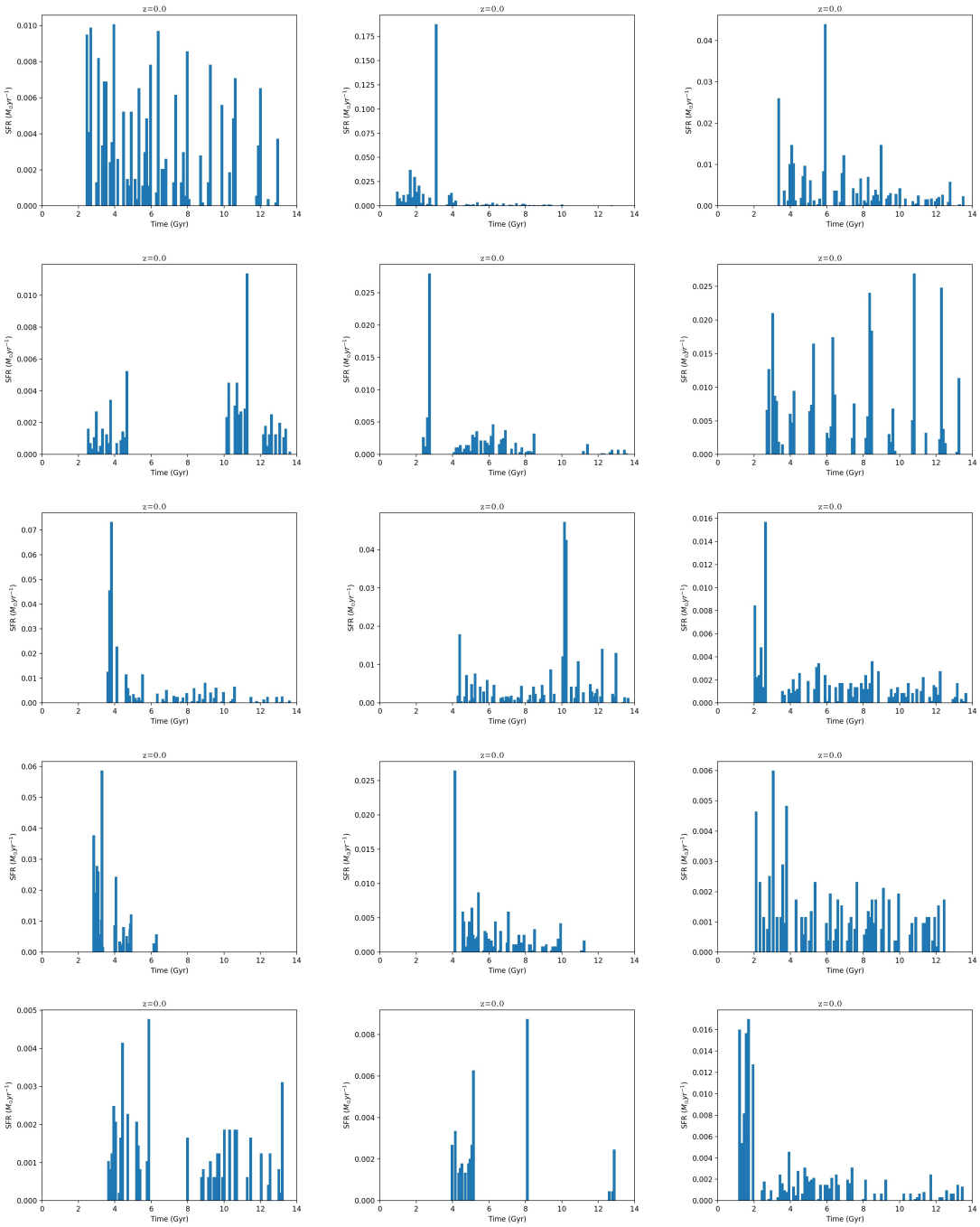
z=0.0
SFR ($M_\odot yr^{-1}$)
Time (Gyr)

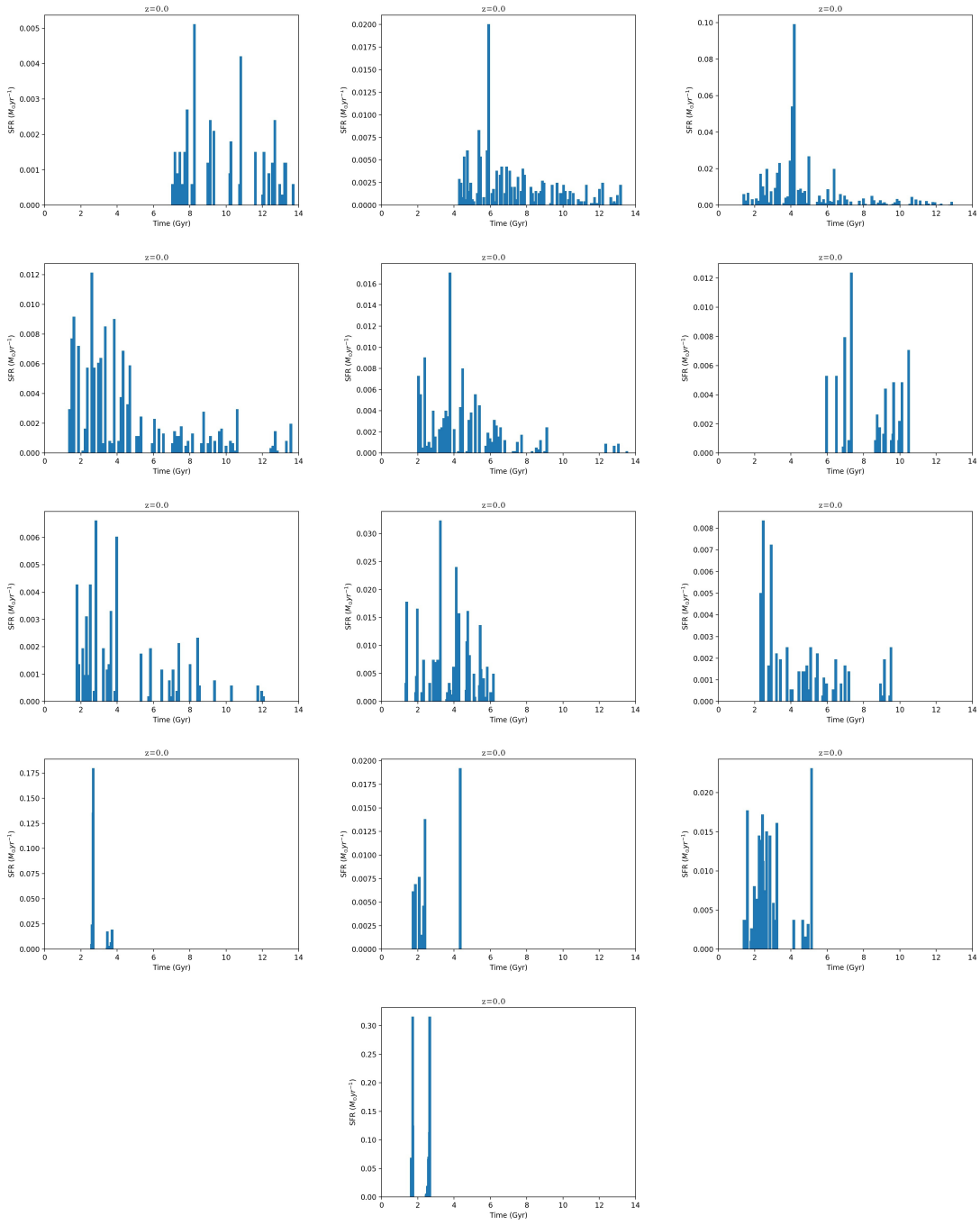

Figure A.3: The rest of the star formation history of our galaxy sample.

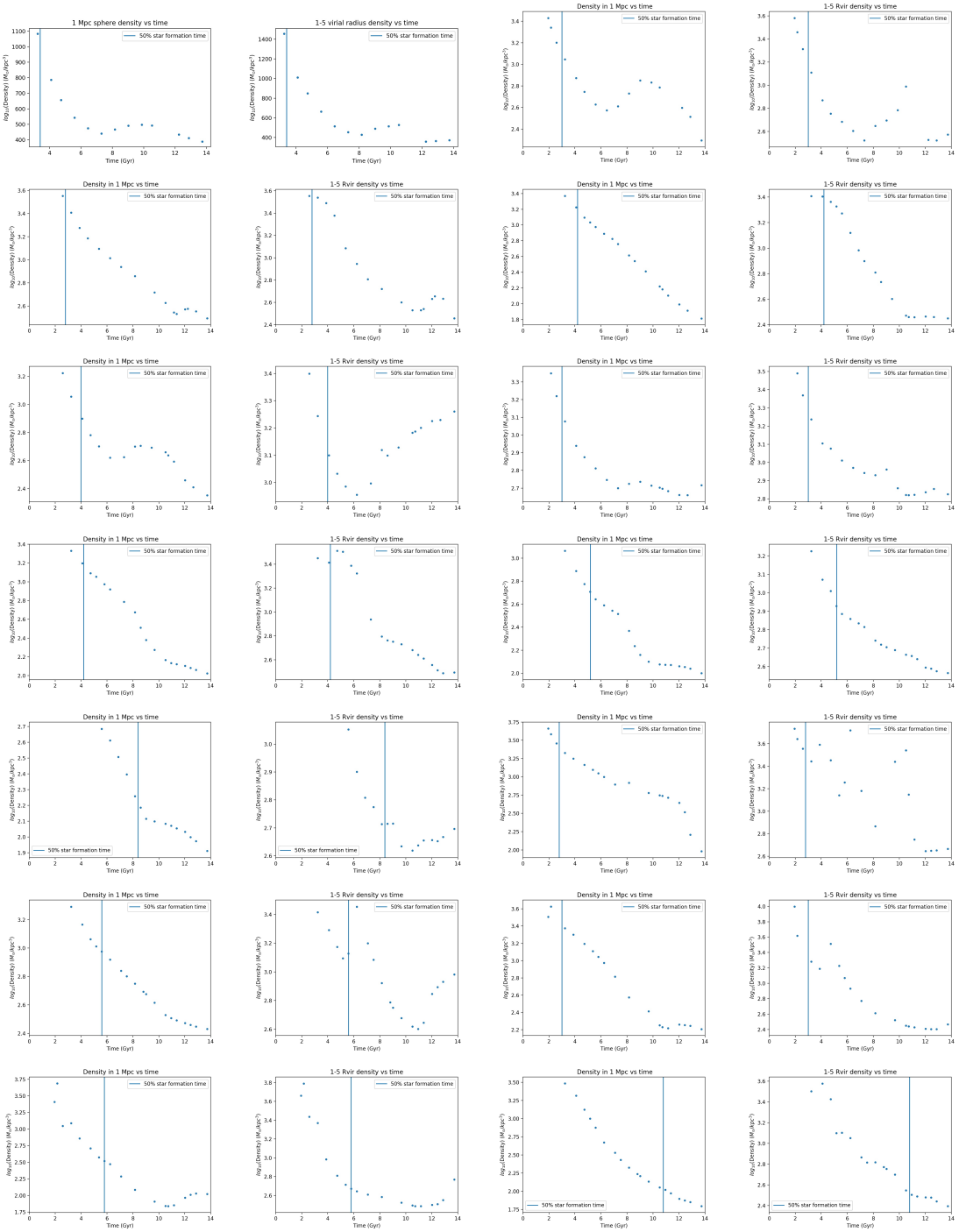
1 Mpc sphere density vs time
1-5 virial radius density vs time
Density in 1 Mpc vs time
1-5 Rvir density vs time
50% star formation time
Time (Gyr)

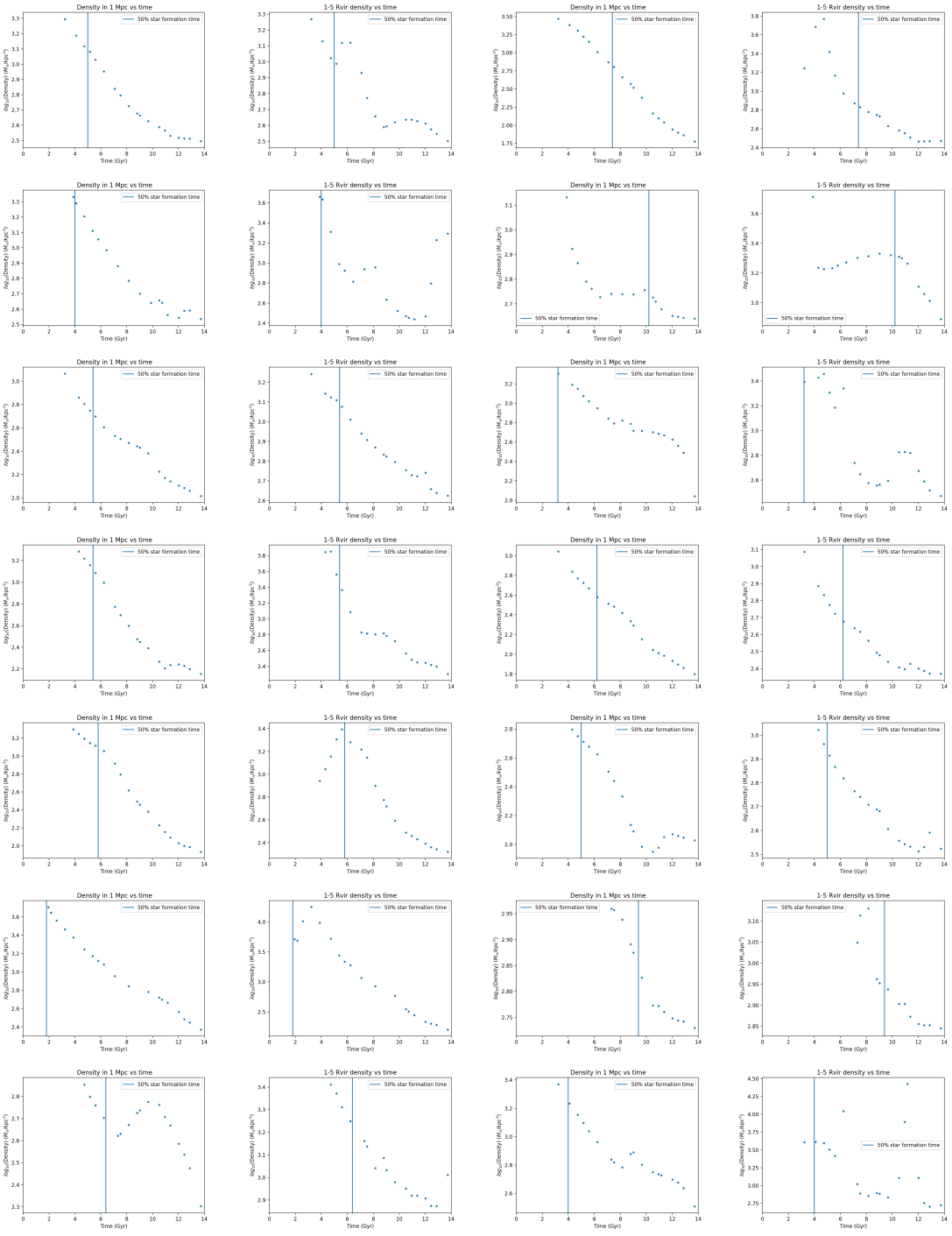
Density in 1 Mpc vs time
1-5 Rvir density vs time
50% star formation time
Time (Gyr)

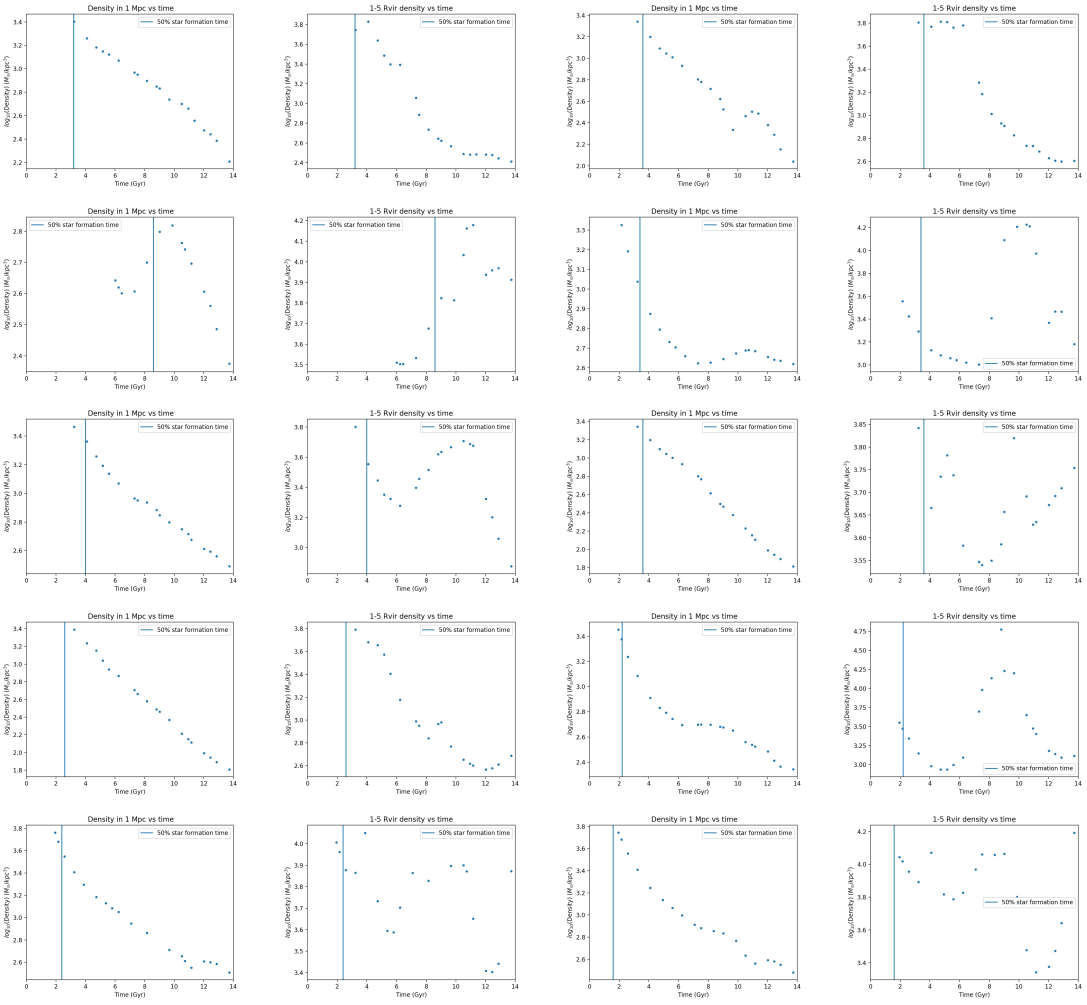

Figure A.6: Density between 1-5 virial radius and inside a sphere of 1 Mpc for the rest of the galaxies of our sample. For each row, the first and second column, and the third and fourth column represent the one galaxy.

References

Gallart, Carme et al. (Sept. 2015). «THE ACS LCID PROJECT: ON THE ORIGIN OF DWARF GALAXY TYPES—A MANIFESTATION OF THE HALO ASSEMBLY BIAS?» In: *The Astrophysical Journal* 811.2, p. L18. DOI: 10.1088/2041-8205/811/2/l18. URL: https://doi.org/10.1088%2F2041-8205%2F811%2F2%2Fl18 (cit. on pp. 1, 2, 10, 12, 25).

Bermejo-Climent, José R et al. (June 2018). «On the early evolution of Local Group dwarf galaxy types: star formation and supernova feedback». In: *Monthly Notices of the Royal Astronomical Society* 479.2, pp. 1514–1527. ISSN: 0035-8711. DOI: 10.1093/mnras/sty1651. eprint: https://academic.oup.com/mnras/article-pdf/479/2/1514/25131796/sty1651.pdf. URL: https://doi.org/10.1093/mnras/sty1651 (cit. on pp. 2, 10, 12–14, 25).

Gottloeber, Stefan, Yehuda Hoffman, and Gustavo Yepes (May 2010). «Constrained Local UniversE Simulations (CLUES)». In: *arXiv e-prints*, arXiv:1005.2687, arXiv:1005.2687. arXiv: 1005.2687 [astro-ph.CO] (cit. on pp. 2, 3, 25).

Peebles, P. J. E. (1998). *The Standard Cosmological Model*. arXiv: astro-ph/9806201 [astro-ph] (cit. on p. 3).

Klypin, Anatoly, Yehuda Hoffman, Andrey V. Kravtsov, and Stefan Gottlober (Oct. 2003). «Constrained Simulations of the Real Universe: The Local Supercluster». In: *The Astrophysical Journal* 596.1, pp. 19–33. DOI: 10.1086/377574. URL: https://doi.org/10.1086%2F377574 (cit. on p. 4).

Willick, Jeffrey A., Stéphane Courteau, S. M. Faber, David Burstein, Avishai Dekel, and Michael A. Strauss (Apr. 1997). «Homogeneous Velocity-Distance Data for Peculiar Velocity Analysis. III. The Mark III Catalog of Galaxy Peculiar Velocities». In: 109.2, pp. 333–366. DOI: 10.1086/312983. arXiv: astro-ph/9610202 [astro-ph] (cit. on p. 4).

Tonry, John L., Alan Dressler, John P. Blakeslee, Edward A. Ajhar, Andre B. Fletcher, Gerard A. Luppino, Mark R. Metzger, and Christopher B. Moore (Jan. 2001). «The SBF Survey of Galaxy Distances. IV. SBF Magnitudes, Colors, and Distances». In: *The Astrophysical Journal* 546.2, pp. 681–693. DOI: 10.1086/318301. URL: https://doi.org/10.1086%2F318301 (cit. on p. 4).

Karachentsev, Igor D., Valentina E. Karachentseva, Walter K. Huchtmeier, and Dmitry I. Makarov (Apr. 2004). «A Catalog of Neighboring Galaxies». In: 127.4, pp. 2031–2068. DOI: 10.1086/382905 (cit. on p. 4).

Reiprich, Thomas H. and Hans Böhringer (Mar. 2002). «The Mass Function of an X-Ray Flux-limited Sample of Galaxy Clusters». In: 567.2, pp. 716–740. DOI: 10.1086/338753. arXiv: astro-ph/0111285 [astro-ph] (cit. on p. 4).

Hoffman, Yehuda and Erez Ribak (Oct. 1991). «Constrained Realizations of Gaussian Fields: A Simple Algorithm». In: 380, p. L5. DOI: 10.1086/186160 (cit. on p. 4).

Santos-Santos, Isabel M., Chris B. Brook, Greg Stinson, Arianna Di Cintio, James Wadsley, Rosa Domínguez-Tenreiro, Stefan Gottlöber, and Gustavo Yepes (Nov. 2015). «The distribution of mass components in simulated disc galaxies». In: *Monthly Notices of the Royal Astronomical Society* 455.1, pp. 476–483. ISSN: 0035-8711. DOI: 10.1093/mnras/stv2335. eprint: https://academic.oup.com/mnras/article-pdf/455/1/476/3084836/stv2335.pdf. URL: https://doi.org/10.1093/mnras/stv2335 (cit. on pp. 4, 7).

Springel, Volker (Dec. 2005). «The cosmological simulation code gadget-2». In: *Monthly Notices of the Royal Astronomical Society* 364.4, pp. 1105–1134. ISSN: 1365-2966. DOI: 10.1111/j.1365-2966.2005.09655.x. URL: http://dx.doi.org/10.1111/j.1365-2966.2005.09655.x (cit. on p. 5).

Wadsley, James W., Benjamin W. Keller, and Thomas R. Quinn (June 2017). «Gasoline2: a modern smoothed particle hydrodynamics code». In: *Monthly Notices of the Royal Astronomical Society* 471.2, pp. 2357–2369. ISSN: 1365-2966. DOI: 10.1093/mnras/stx1643. URL: http://dx.doi.org/10.1093/mnras/stx1643 (cit. on p. 5).

Governato, F. et al. (Jan. 2010). «Bulgeless dwarf galaxies and dark matter cores from supernova-driven outflows». In: 463.7278, pp. 203–206. DOI: 10.1038/nature08640. arXiv: 0911.2237 [astro-ph.CO] (cit. on p. 7).

Haardt, Francesco and Piero Madau (Apr. 1996). «Radiative Transfer in a Clumpy Universe. II. The Ultraviolet Extragalactic Background». In: 461, p. 20. DOI: 10.1086/177035. arXiv: astro-ph/9509093 [astro-ph] (cit. on p. 7).